

generally not related to the surface topography. Figure 4 shows a comparison of the temperature dependence of the CMR ratio $[R(0\text{ T}) - R(9\text{ T})]/R(9\text{ T})$, where R is the sample resistance, with the relative change in image brightness as determined from STS images similar to Fig. 3 in 0 and 9 T. There is excellent agreement between the temperature-dependent field sensitivity of our STS data and the magnetoresistive properties. This makes us confident that the tunneling measurements at the sample surface are representative for the bulk behavior and that the spectroscopic images can be regarded as two-dimensional cross sections of the three-dimensional sample volume.

The observations of the MIT and its spatial variations in the tunneling spectra are qualitatively the same for the various types of samples investigated. The cloudlike patterns signify static electronic inhomogeneities, which imply the existence of regions with different Mn oxidation states, meaning hole concentration. However, the phase separation is not as clear as in the case of $\text{La}_{0.5}\text{Ca}_{0.5}\text{MnO}_3$, where microdomains of a charge-ordered phase can be observed (15). Here, the phases do not appear to be fully metallic nor fully insulating, which might be a precursor to full separation. The origin of the observed phase separation is not yet clear, especially because at our doping concentration a homogeneous low-temperature state might be expected, with a dynamic rather than a static tendency for separation (4). It seems likely that structural disorder destroys the fragile balance in the system, which would help to explain the large length scales. Variations in the oxygen content are one possibility. Twinning is another; in both crystals, strong twinning on length scales of <100 nm was clearly observed by HREM (16). Such subtle disorder effects are unavoidable, even in state-of-the-art material; they should be taken into account in the interpretation of all current experiments and, in that sense, are an intrinsic part of the physics of the manganites. In this specific framework, our STS results force us to view the CMR as a magnetization-dependent phase separation that percolates, thereby generating a MIT.

References and Notes

- C. Zener, *Phys. Rev.* **82**, 403 (1951).
- A. J. Millis, *Nature* **392**, 147 (1998).
- R. Maezono, S. Ishihara, N. Nagaosa, *Phys. Rev. B* **58**, 11583 (1998).
- A. Moreo, S. Yunoki, E. Dagotto, *Science* **283**, 2034 (1999), and references therein.
- R. H. Heffner *et al.*, *Phys. Rev. Lett.* **77**, 1869 (1996).
- C. H. Booth *et al.*, *Phys. Rev. B* **57**, 10440 (1998).
- S. Yoon *et al.*, *ibid.* **58**, 2795 (1998); H. L. Liu *et al.*, *ibid.*, p. R10115.
- J. W. Lynn *et al.*, *Phys. Rev. Lett.* **76**, 4046 (1996).
- J. M. De Teresa *et al.*, *Nature* **386**, 256 (1997).
- A. Lanzara *et al.*, *Phys. Rev. Lett.* **81**, 878 (1998).
- S. Frisem *et al.*, *J. Magn. Magn. Mater.* **165**, 380 (1997); J. Aarts *et al.*, *Appl. Phys. Lett.* **72**, 2975 (1998).
- J.-H. Park *et al.*, *Phys. Rev. Lett.* **76**, 4215 (1996).
- J. Y. T. Wei, N.-C. Yeh, R. P. Vasquez, *ibid.* **79**, 5150 (1997).
- J. M. D. Coey, M. Viret, L. Ranno, *ibid.* **75**, 3910 (1995).
- S. Mori, C. H. Chen, S.-W. Cheong, *ibid.* **81**, 3972 (1998).
- H. W. Zandbergen, private communication.
- We gratefully acknowledge discussions with J. Zaanen, D. Khomskii, A. Millis, and Y. Tokura. The work is supported in part by the Dutch Foundation for Fundamental Research of Matter (FOM) and by the New Energy and Industrial Technology Development Organization (NEDO) of Japan.

6 May 1999; accepted 19 July 1999

Stable Five- and Six-Coordinated Silicate Anions in Aqueous Solution

Stephen D. Kinrade,^{1*} Jeffrey W. Del Nin,¹ Andrew S. Schach,¹ Todd A. Sloan,¹ Krista L. Wilson,¹ Christopher T. G. Knight²

Addition of aliphatic polyols to aqueous silicate solutions is shown to yield high concentrations of stable polyolate complexes containing five- or six-coordinated silicon. Coordinating polyols require at least four hydroxy groups, two of which must be in *threo* configuration, and coordinate to silicon via hydroxy oxygens at chain positions on either side of the *threo* pair. The remarkable ease by which these simple sugar-like molecules react to form hypervalent silicon complexes in aqueous solution supports a long-standing supposition that such species play a significant role in the biological uptake and transport of silicon and in mineral diagenesis.

The chemistry of silicon in the natural world is dominated by its affinity for oxygen, to which it is almost always tetrahedrally coordinated. Reports of naturally occurring pentaoxo- and hexaoxosilicon centers are very rare. In silicate minerals, five-coordinate centers are completely unknown, whereas six-coordinated silicon only occurs in high-pressure phases such as stishovite (1). In synthetic crystalline materials (including zeolite molecular sieves), only tetrahedral Si sites have been reported in cases where all coordinating atoms are oxygen. Silicate glasses are unique, however, in that they can contain silicon coordinated to four, five, or six oxygens, even when formed at atmospheric pressure, although the four-coordinate center remains by far the most common (2). A number of synthetic organosilicate complexes have been reported to contain hypervalent silicon (3–9). For example, mono- and dimeric pentacoordinate silicon glycolates form on dissolution of silica in ethylene glycol with an alkali-metal base (3, 4), and are implicated as intermediates in the nonaqueous synthesis of zeolites (6). The corresponding hexaalkoxy-silicate species result when a group II metal oxide is used in place of the alkali-metal base (5). In aqueous solution, pentaoxosilicon is

unknown and the hexaoxo-center is documented only for complexes in which silicon is chelated by catechol (yielding tris[1,2-benzenediolato]silicate) (10), 2-hydroxypyridine *N*-oxide (11), tropolone (12), or closely related analogs.

In an attempt to understand, on a molecular level, the formation of zeolites and microporous materials, we have studied the effects of alcohols and simple organic cations on the structure of aqueous silicate anions using ²⁹Si nuclear magnetic resonance (NMR) spectroscopy (13). We have observed in the course of this work that the addition of alkyl 1,2-diols to aqueous silicate solutions produces low concentrations of silicon-diolate complexes giving ²⁹Si NMR signals around –102 parts per million (ppm). These peaks closely correspond to those that Blohowiak *et al.* (4) and Herreros *et al.* (6) assign to five-coordinated silicon tris-glycolate complexes in H₂O-free ethylene glycol. However, the low concentrations of the complexes in aqueous solution prevent further structural refinement.

We report here that certain aliphatic polyhydroxy alcohols readily yield solutions containing high concentrations of stable hypervalent silicate anions. The silicon in these polyolate complexes can be in either five- or sixfold coordination by oxygen. The complexes are so stable that under favorable conditions they dominate the equilibrium, sometimes to the exclusion of the usual four-coordinate silicate species. In 11.7-T, ²⁹Si NMR spectra of a sodium silicate solution containing xylitol, three main peaks are noted

¹Department of Chemistry, Lakehead University, 955 Oliver Road, Thunder Bay, Ontario, Canada P7B 5E1.

²School of Chemical Sciences, University of Illinois at Urbana-Champaign, 600 South Mathews Avenue, Urbana, IL 61801, USA.

*To whom correspondence should be addressed. E-mail: Stephen.Kinrade@lakeheadu.ca

at -71 , -102 , and -144 ppm (Fig. 1A). Comparison to the chemical shifts of well-characterized silicates in the literature (2–12) indicates that these signals must arise from silicate anions in, respectively, four-, five-, and sixfold coordination by oxygen. The peak at -71 ppm is clearly that of the monomeric silicate anion, Q^0 (13, 14). The spectrum of an identical solution to which sufficient NaOH has been added to bring the $[\text{NaOH}]:[\text{SiO}_2]$ concentration ratio up to 2.5:1 consists almost exclusively of one signal at -144 ppm (Fig. 1B), demonstrating that the majority of silicon in solution exists as a hexavalent polyolate complex. The changes are completely reversible with pH, and the solutions are stable with time. Figure 2 shows similar results for solutions containing an equivalent concentration of the smaller polyhydroxy additive, threitol, although the overall extent of complexation is less.

Such high coordination polyolate complexes only form in significant quantities when the aliphatic polyol additive has four or more adjacent hydroxy groups, with two being in *threo* configuration (15). Thus, of the polyols shown in Fig. 3, threitol, arabitol, galactitol, mannitol, sorbitol, and xylitol all yield high concentrations of polyolate complexes, whereas *meso*-erythritol and adonitol do not. Additionally, we note that the polyols which favor complexation also enhance silica solubility, and as a consequence, allow the

preparation of low ratio ($[\text{OH}^-]:[\text{SiO}_2] < 1:1$) solutions containing up to 3 mol liter $^{-1}$ SiO_2 without sample gelling, even in the presence of alkali metal cations.

Determining the structure of these high-coordination silicon complexes is not straightforward. Herreros *et al.* (6) proposed that the major solution species in H_2O -free ethylene glycol, which yields a ^{29}Si NMR peak at -105.5 ppm, is a fully encapsulated binary tris-silicoglycolate complex in which each silicon is coordinated to two ethylene glycol ligands and shares a third. However, their assignment is based solely on the chemical shift of the well characterized crystalline solid, at -102.7 ppm, and must be regarded as tentative.

Close examination of our ^{29}Si NMR spectra reveals the simultaneous presence of multiple signals in both the five- and six-coordinate regions (Figs. 1, 2, 4, and 5). Moreover, the signals show evidence of long-range scalar coupling to protons. Because of the aqueous nature of the samples, rapid chemical exchange would normally ensure that no hydroxy proton coupling is seen in the ^{29}Si NMR spectrum. Consequently, the observed ^{29}Si - ^1H coupling must involve the aliphatic protons of the polyol. This implies a formal covalent Si-O-C-H linkage, and indicates that at least one polyol is directly bound to silicon in these species. Furthermore, the ^{29}Si NMR signals do not exhibit any ^{29}Si - ^{29}Si coupling for solutions prepared with silica enriched in

silicon-29. They must therefore arise from species that contain only a single silicon chemical environment, suggesting in the simplest case a monomeric silicate species, the various signals arising from differences in either the number of bound polyol groups or the position or manner in which they bind.

In low alkalinity polyolate solutions, with $[\text{OH}^-]:[\text{SiO}_2]$ ratios of one or less, five-coordinate anions dominate the equilibrium. Carbon-13 NMR spectroscopy reveals that polyols coordinate to silicon primarily through the hydroxy oxygens of the two carbons at either side of the *threo* hydroxy pair

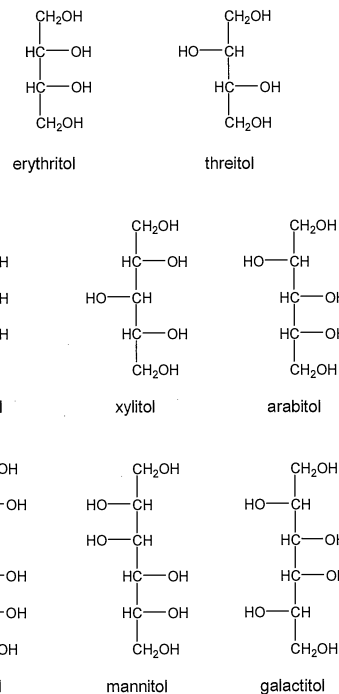


Fig. 3. Fischer projections of the aliphatic polyhydroxy molecules used in the present study. All except erythritol and adonitol readily complex with aqueous silicate anions.

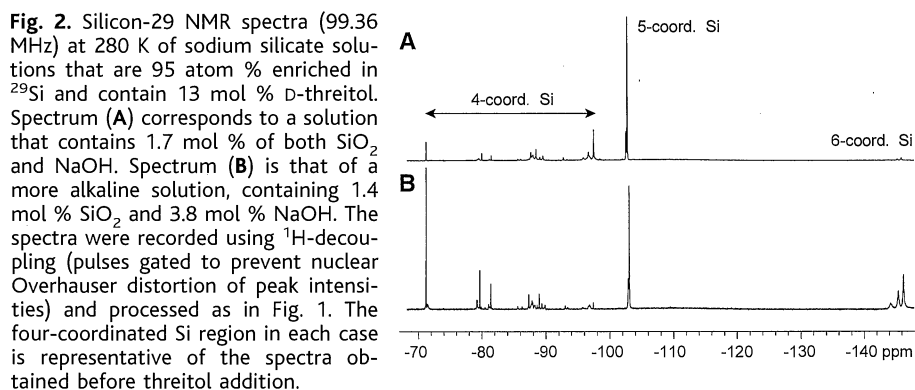
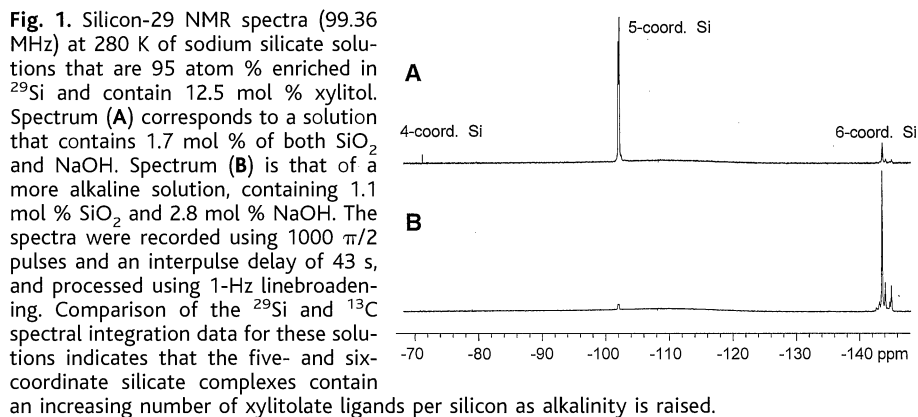


Fig. 2. Silicon-29 NMR spectra (99.36 MHz) at 280 K of sodium silicate solutions that are 95 atom % enriched in ^{29}Si and contain 13 mol % D-threitol. Spectrum (A) corresponds to a solution that contains 1.7 mol % of both SiO_2 and NaOH. Spectrum (B) is that of a more alkaline solution, containing 1.4 mol % SiO_2 and 3.8 mol % NaOH. The spectra were recorded using ^1H -decoupling (pulses gated to prevent nuclear Overhauser distortion of peak intensities) and processed as in Fig. 1. The four-coordinated Si region in each case is representative of the spectra obtained before threitol addition.

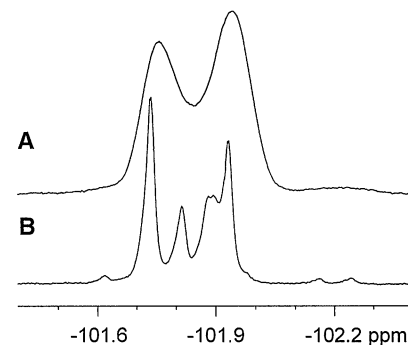


Fig. 4. Spectrum (A) is an expansion of the region that is characteristic of five-coordinated Si in the ^1H -coupled ^{29}Si NMR spectrum shown in Fig. 1A. Comparison with spectrum (B), the corresponding ^1H -decoupled (gated) spectrum, reveals the existence of Si-O-C-H covalent bonding in silicon xylitolate complexes.

(16). Thus for arabinol, galactitol, sorbitol, threitol and xylitol, all of which have the *threo* pair at carbons 2 and 3 (Fig. 3), the primary Si coordination sites are the oxygens of carbons 1 and 4. In the case of mannitol, the *threo* hydroxy pair is located at carbons 3 and 4 (Fig. 3) causing the Si coordination sites to move to the oxygens at carbons 2 and 5 (16, 17).

As the solution alkalinity is raised, a second set of ^{13}C NMR signals appears (18). These are attributable to increased deprotonation of the silicate centers (19). Integration of the ^{13}C and ^{29}Si NMR spectra reveals that the average number of polyols per complex does indeed increase, apparently toward a maximum of two.

Molecular models incorporating standard covalent bond angles and lengths indicate that the polyols giving optimal complex formation are ones which can easily wrap themselves around a silicate anion. Modeling also suggests that the complexes are stabilized by hydrogen bonding (possibly solvent mediated) between the uncoordinated polyol hydroxy groups and the silicate anion hydroxy groups. Because the hydroxy groups of the complexing polyol are directed toward the silicate center, the hydrophobic character of its outward-facing hydrocarbon backbone may well protect the resulting polyolate complex from hydrolysis. The reaction schemes

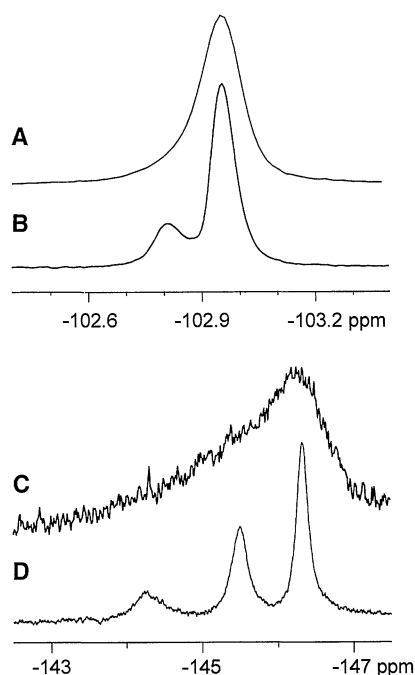


Fig. 5. Spectrum (A) is an expansion of the five-coordinated Si region in Fig. 2A, but with no ^1H -decoupling. Spectrum (B) is the identical spectrum obtained using gated ^1H -decoupling. Spectrum (C) is an expansion of the six-coordinated Si region in Fig. 2B, but with no ^1H -decoupling. Spectrum (D) is the corresponding decoupled spectrum.

that can be derived from the combined NMR data (Fig. 6) are consistent with ^{29}Si NMR observations in showing that only five-coordinated silicate complexes can exist in very low alkalinity solutions, that is, when silicic acid is strictly monodeprotonated [$q = 1$ in $(\text{HO})_{4-q}\text{SiO}_q^{q-}$]. Increasing pH, and thus the extent of deprotonation, permits formation of the hexa-coordinated complexes. The reaction schemes also show that 1:2 silicate-polyol complexes form at the expense of the 1:1 complexes with a rise in polyol concentration or pH, as born out by the ^{13}C and ^{29}Si integration data.

Many naturally occurring organic molecules and substrates, including cellular surfaces, contain groups structurally similar to the simple polyols that were used here. Thus, such hypervalent silicate complexes may play a vital role in the solution chemistry of sili-

con, from the dissolution and formation of silicate minerals to the transport and mineralization of silicon in the biosphere. Limited evidence exists on how silicon is isolated, transported and deposited by simple plants and animals, although complexing by sugars has long been suspected (20). However, Birchall (21) observed that "... no fundamental biochemical function has been defined and no stable organic binding has been demonstrated for silicon. ... There is no evidence of strong interactions between silicic acid and cis-diols in sugars for example. ... The presence of Si-O-C bonds has not been demonstrated and is unlikely." Our observation of the ease by which silicon binds to polyols of the appropriate structural configuration would suggest that polyhydroxy containing groups and surfaces may indeed play a key role in isolating silica and silicic acids in nature.

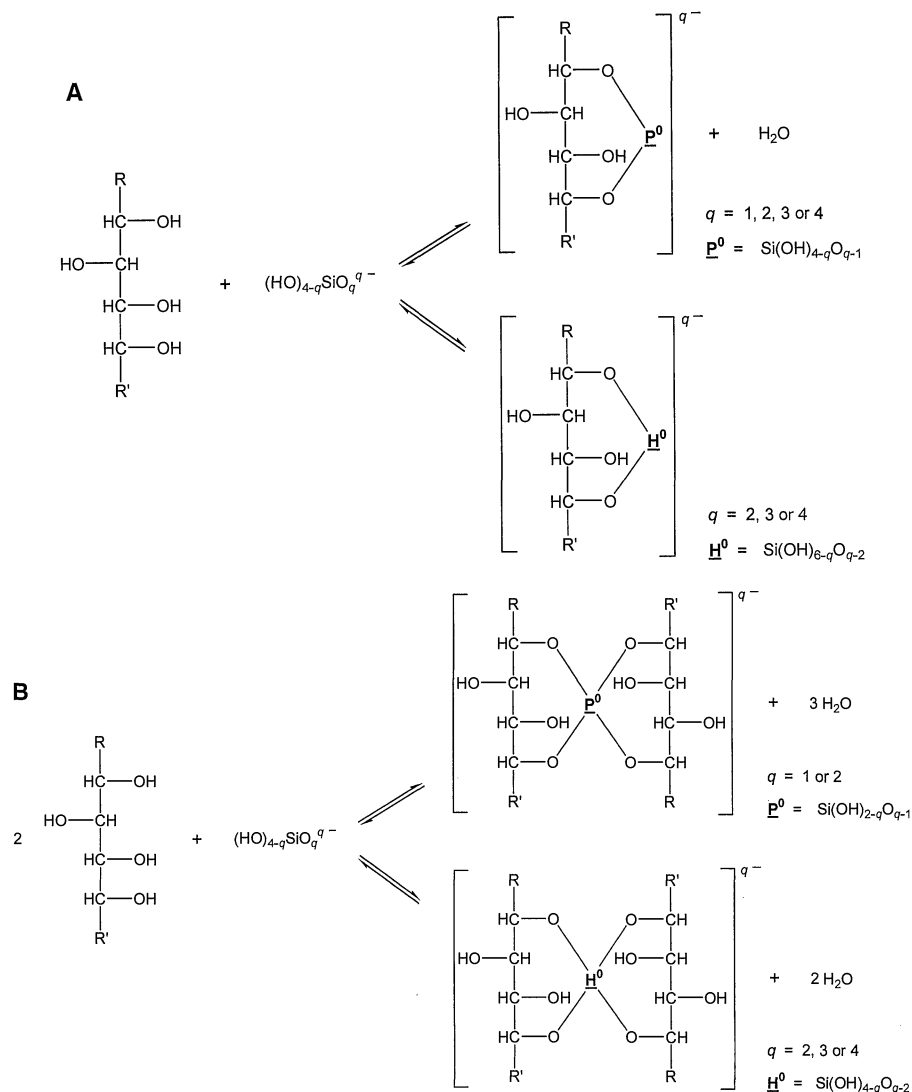


Fig. 6. Reaction schemes for the formation of silicon polyolate complexes. R and R' represent polyol chain ends— $(\text{CHOH})_n\text{H}$, where $n \geq 0$. The extent of deprotonation q of the silicic acid monomer $[(\text{HO})_{4-q}\text{SiO}_q^{q-}]$ is 1 on average for solutions with $[\text{OH}^-]:[\text{Si}] = 1:1$, and increases with solution alkalinity (19). Refer to (14) for the nomenclature of silicate centers.

References and Notes

1. F. Liebau, *Structural Chemistry of Silicates* (Springer-Verlag, Berlin, 1985).
2. J. F. Stebbins and P. F. McMillan, *J. Non-Cryst. Solids* **160**, 116 (1993); *Am. Mineral.* **74**, 965 (1989).
3. R. M. Laine *et al.*, *Nature* **353**, 642 (1991); *J. Mater. Chem.* **6**, 1441 (1996).
4. K. Y. Blohowiak *et al.*, *Chem. Mater.* **6**, 2177 (1994).
5. M. L. Hoppe, R. M. Laine, J. Kampf, M. S. Gordon, L. W. Burggraf, *Angew. Chem. Int. Ed. Engl.* **32**, 287 (1993).
6. B. Herreros, S. W. Carr, J. Klinowski, *Science* **263**, 1585 (1994).
7. C. Chuit, R. J. P. Corriu, C. Reyé, J. C. Young, *Chem. Rev.* **93**, 1371 (1993).
8. G. J. Gainsford, T. Kemmitt, N. B. Milestone, *Acta Crystallogr. C* **51**, 8 (1995); T. Kemmitt and N. B. Milestone, *Aust. J. Chem.* **48**, 93 (1995).
9. J. H. Small, K. J. Shea, D. A. Loy, G. M. Jamison, *ACS Symp. Ser.* **585**, 248 (1995).
10. A. Rosenheim, B. Reibmann, G. Schendel, *Z. Anorg. Chem.* **196**, 160 (1931); I. F. Sedeh, S. Sjöberg, L. O. Öhman, *Acta Chem. Scand.* **46**, 933 (1992); *J. Inorg. Biochem.* **50**, 119 (1993).
11. A. Weiss and D. R. Harvey, *Angew. Chem.* **76**, 818 (1964).
12. S. Sjöberg, N. Ingri, A. M. Nenner, L. O. Öhman, *J. Inorg. Biochem.* **24**, 267 (1985); D. F. Evans, J. Parr, C. Y. Wong, *Polyhedron* **11**, 567 (1992).
13. S. D. Kinrade, K. J. Maa, A. S. Schach, T. A. Sloan, C. T. G. Knight, *J. Chem. Soc. Dalton Trans.*, in press; S. D. Kinrade, C. T. G. Knight, D. L. Pole, R. T. Syvitski, *Inorg. Chem.* **37**, 4272 (1998); *ibid.*, p. 4278; C. T. G. Knight, *Zeolites* **9**, 448 (1989).
14. It has become accepted in the literature that four-coordinate silicate centers are denoted by a "Q" for quadrifunctional. The extent of protonation is ignored, and a superscript is used to indicate the number of shared siloxane linkages. Choosing symbols for the five- and six-coordinate centers that are, at once, systematic and practical to use is difficult. The Latin prefix quinti- presents an obvious problem. Herreros *et al.* (6) used a Roman superscript to indicate five-coordinate sites, for example Si^V, but such a system becomes unwieldy describing other than symmetric silicate species. We propose using Greek prefixes to describe the state of Si coordination, obtaining "P" for pentafunctional and "H" for hexafunctional. This terminology is immediately understandable and avoids use of unusual typographical symbols. Over- or underscoring the labels is recommended to avoid confusion with the corresponding elements. Thus, the monomeric species represented by the resonances in Fig. 1 would be labeled as Q⁰, P⁰, and H⁰.
15. That is, only when there are two adjacent hydroxy groups occurring on opposite sides of the molecule's Fischer projection (Fig. 3).
16. For low-alkalinity solutions ([OH⁻]:[SiO₂] ≤ 1:1), the ¹³C NMR signals corresponding to Si-coordination sites on the polyol shift up-frequency by 1 to 3 ppm from their bulk solution values. Thus, whereas free D-threitol resonates at 62.9 (C-1,4) and 71.8 ppm (C-2,3), the major threitol-Si complex resonates at 64.7, 64.9 (-OSi coordinated C-1,4), 70.7, and 71.7 ppm (C-2,3). Similarly, only the C-2,5 signals of D-mannitol move up-frequency upon silicate complexation, shifting from 71.4 ppm to 74.2 and 74.5 ppm.
17. Carbon-13 NMR investigations into the interaction between aqueous borates and polyols reveal similar high-frequency shifts upon complex formation [A. Munoz and L. Lamandé, *Carbohydrate Res.* **225**, 113 (1991)]. Consistent with our observations, the structural criterion for optimal borate complex formation appears to be that the polyols contain a *threo* hydroxy pair. However, the boron center appears to bind across the *threo* pair itself, rather than at sites adjacent to it. Moreover, boron does not undergo an increase in coordination number.
18. As the [OH⁻]:[SiO₂] ratio of solutions containing D-threitol is raised above 1:1, new ¹³C NMR signals occur at 66.0 (C-1,4) and 70.2 ppm (C-2,3).
19. S. D. Kinrade, *J. Phys. Chem.* **100**, 4760 (1996); I. L. Svensson, S. Sjöberg, L.-O. Öhman, *J. Chem. Soc. Faraday Trans.* **31**, 4558 (1989).
20. J. J. R. Frausto da Silva and R. P. J. Williams, *The Biological Chemistry of the Elements* (Clarendon, Oxford, 1991); R. K. Iler, *The Chemistry of Silica* (Wiley, New York, 1979).
21. J. D. Birchall, *Chem. Soc. Rev.* **24**, 351 (1995).
22. We thank J. T. Banks for helpful discussions and R. J. Kirkpatrick for the generous loan of isotopically enriched silica. Funding was provided in part by NIH (PHS 1 S10 RR 10444-01; GM-42208 and RR 01811), NSF (NSF CHE 96-10502), and the Natural Sciences and Engineering Council of Canada (NSERC). Facilities were provided by the NIH-supported Illinois EPR Research Center, and the NSERC-supported Prairie Regional NMR Centre (Winnipeg).

23 February 1999; accepted 15 July 1999

Seismic Velocity and Density Jumps Across the 410- and 660-Kilometer Discontinuities

Peter M. Shearer^{1*} and Megan P. Flanagan²

The average seismic velocity and density jumps across the 410- and 660-kilometer discontinuities in the upper mantle were determined by modeling the observed range dependence in long-period seismic wave arrivals that reflect off of these interfaces. The preliminary reference Earth model (PREM) is within the computed 95 percent confidence ellipse for the 410-km discontinuity but outside the allowed jumps across the 660-kilometer discontinuity. Current pyrolite mantle models appear consistent with the constraints for the 410-kilometer discontinuity but overpredict amplitudes for the 660-kilometer reflections. The density jump across the 660-kilometer discontinuity is between 4 and 6 percent, below the PREM value of 9.3 percent commonly used in mantle convection calculations.

Observed seismic velocity discontinuities near 410- and 660-km depth in Earth's upper mantle are believed to be caused primarily by phase changes in olivine and other minerals that result from the increasing pressure with increasing depth (1). Resolving the details of the discontinuities is important for modeling the composition of the mantle and for understanding the effect that the discontinuities may have on mantle convection (2). Recent analyses of reflected seismic phases (3–5) have yielded estimates of the average discontinuity depths that agree within ±1%; in contrast, the average *P* and *S* velocity increases across the boundaries are known less precisely, and differences of a factor of 2 or greater are seen in the velocity jumps obtained in different studies (6). The density jumps, critical parameters for modeling of mantle dynamics, are particularly hard to measure and are often based on velocity versus density scaling relations rather than direct observational measurements.

In principle, however, the velocity and density jumps can be separately resolved by studying the behavior of reflection coefficients (7) as a function of ray angle. Following this approach, we used the observed amplitudes of reflections off the bottom of the 410- and 660-

km discontinuities to measure the velocity and density jumps across the interfaces. These reflections occur as precursors to the phases *SS* and *PP* in long-period seismograms (8). Our data consisted of 13,469 transverse-component and 24,667 vertical-component seismograms from the global seismic networks (GDSN, IRIS, and Geoscope) recorded between 1976 and 1997. To enhance the visibility of the discontinuity reflections, we aligned the seismograms on the maximum amplitude of *SS* (for the transverse components) and *PP* (for the vertical components) and stacked the data in bins of constant source-receiver range (Fig. 1). The underside reflected phases *S410S* and *S660S* were visible in the transverse-component stack, arriving 2 to 4 min before the direct *SS* phase. The underside *P* reflection off the 410-km discontinuity, *P410P*, was observed in the vertical-component stack between 100° and 145°, but the underside 660-km reflection, *P660P*, was not seen (9, 10). Additional details concerning the data and our stacking methods may be found in previous studies (4, 11, 12).

We measured the relative amplitudes between the discontinuity reflections and the reference phases *SS* and *PP* within 1° bins in source-receiver distance across the intervals for which arrivals were visible (112° to 160° for *S410S*, 118° to 165° for *S660S*, and 102° to 140° for *P410P*). Because of interference from *PKP*, we did not use *P410P* data between 118° and 130°. Although *P660P* was not visible, limits could still be placed on its average amplitude between 118° and 122°, where interference from other phases is ab-

¹Institute of Geophysics and Planetary Physics, Scripps Institution of Oceanography, University of California, San Diego, La Jolla, CA 92093–0225, USA.

²Lawrence Livermore National Laboratory, Post Office Box 808, L-206, Livermore, CA 94551, USA.

*To whom correspondence should be addressed.